PERGAMON

International Journal of Multiphase Flow 24 (1998) 739–755

International Journal of Multiphase Flow

Transient simulation of two-phase flows in pipes

J.M. Masella, Q.H. Tran, D. Ferre, C. Pauchon

Institut Français du Pétrole, B.P. 311, 92852 Rueil-Malmaison Cedex, France

Received 18 February 1997; received in revised form 19 January 1998

Abstract

Transient simulation of two-phase gas-liquid flow in pipes requires considerable computational efforts. Until recently, most available commercial codes are based on the two-fluid model which includes one momentum conservation equation for each phase. However, in normal pipe flow operation, especially in oil and gas transport, the transient response of the system proves to be relatively slow. Thus it is reasonable to think that simpler forms of the transport equations might suffice to represent transient phenomena. Furthermore, these types of models may be solved using less time-consuming numerical algorithms. © 1998 Elsevier Science Ltd. All rights reserved.

Keywords: Two-phase flow; Severe slugging; Acoustic waves; Void fraction

1. Introduction

Transient simulations of gas-liquid flow in pipelines involves elaborate computer codes, the design and use of which demand tremendous efforts. Several codes have been proposed so far, supported by oil and gas industry. Historically, OLGA is the first ever of these. Developed in Norway (Bendiksen et al., 1987, 1991), OLGA is a two-fluid model with an additional momentum equation for the droplet field. The PLAC code (Black et al., 1990), born in England a few years later, is also a two-fluid model. At the Institut Français du Pétrole, another approach based on drift flux type models has been taken. The resulting code TACITE is meant to become a commercial product (Pauchon et al., 1993, 1994). In the drift flux side, there has to be mentioned TRAFLOW, a product developed by the Shell Oil Company.

In the case of OLGA and PLAC, the model development and resolution algorithms had been initiated earlier by the nuclear industry. In the nuclear industry, fast transients associated to Loss Of Coolant Accidents (LOCA) are of major interest, while in the oil and gas industry, the interest often lies in relatively slow transients, associated to the transport and subsequent release of slugs at receiving facilities. Under these conditions, one may consider the momentum

PII: S0301-9322(98)00004-4

equation to be a steady state force balance, thus leading to simpler and less elaborate calculations. Taitel et al. (1989) put forward a simplified model in which the gas mass flow rate is declared to be in steady state. Unfortunately, this approach lacked the ability to account for the transport time along the line in the case of gas flowrate variation at the inlet.

In this paper, we wish to study the behavior of various types of models under a few transient scenarios. Three different models were implemented, namely:

- a Two Fluid Model (TFM), based on one momentum conservation equation for each phase;
- a Drift Flux Model (DFM), based on one momentum conservation equation and an algebraic slip relation;
- a No Pressure Wave (NPW) model, based on an algebraic relation for the pressure drop and an algebraic slip relation.

It has to be expected that these three models have very different analytical properties. For instance, while TFM and DFM are hyperbolic models, the NPW model is a mixed parabolic/hyperbolic one. Therefore, the numerical schemes in use will be different from one model to another.

In a first stage, we seek to analyze the differences in response due solely to the model equations. For the purpose of our study, the pipeline is visualized as a 1–D element of length L. The coordinate along the pipe is called x. We also assume that the pipe properties such as inclination θ with respect the horizontal, diameter D, roughness, etc. are constant along x. Temperature is constant as well, and no mass transfer occurs between the two phases. The response of the three transport models are compared against selected transient scenarios, which exemplify typical operational transient scenarios.

In a second stage, we look at the three codes from the standpoint of computing efficiency. The latter reflects the trade-off between computing time and accuracy of the model response. As for accuracy, it is defined in terms of the operating variables which are most significant for the end user, that is, the peak in outlet liquid flowrate subsequent to an increase in the inlet gas flowrate.

2. The two-fluid model

In dispersed flow, the contrast between the two phasic velocities is small. Understandably, it is anticipated that the added value of the two-fluid model will be more apparent in the stratified regime. This is why we shall rather emphasize the stratified configuration in our presentation of TFM.

2.1. Transport equations

TFM is governed by a set of four partial differential equations, the first two of which express mass conservation

$$\frac{\partial}{\partial t}[\rho_G R_G] + \frac{\partial}{\partial x}[\rho_G R_G V_G] = 0 \tag{1}$$

$$\frac{\partial}{\partial t}[\rho_L R_L] + \frac{\partial}{\partial x}[\rho_L R_L V_L] = 0, \tag{2}$$

and the last two of which represent momentum balance

$$\frac{\partial}{\partial t}[\rho_G R_G V_G] + \frac{\partial}{\partial x}[\rho_G R_G V_G^2 + R_G \Delta P_G] + R_G \frac{\partial}{\partial x} P = \tau_G + \tau_i - \rho_G g \sin\theta \tag{3}$$

$$\frac{\partial}{\partial t}[\rho_L R_L V_L] + \frac{\partial}{\partial x}[\rho_L R_L V_L^2 + R_L \Delta P_L] + R_L \frac{\partial}{\partial x} P = \tau_L - \tau_i - \rho_L g \sin\theta \tag{4}$$

In Eq. (3) and equ. (4), P denotes the interface pressure, while V_k, ρ_k and R_k are respectively the velocity, the density and the volume fraction of phase $k \in \{G,L\}$. The variables τ_i and τ_k are the interfacial and wall momentum exchange terms. The quantities ΔP_G and ΔP_L correspond to static head around the interface (De Henau and Raithby, 1995), defined as

$$\Delta P_G = P_G - P = -\rho_G \left[\frac{1}{2} \cos\left(\frac{\omega}{2}\right) + \frac{1}{3\pi R_G} \sin^3\left(\frac{\omega}{2}\right) \right] g D \cos\theta \tag{5}$$

$$\Delta P_L = P_L - P = -\rho_L \left[\frac{1}{2} \cos\left(\frac{\omega}{2}\right) + \frac{1}{3\pi R_L} \sin^3\left(\frac{\omega}{2}\right) \right] g D \cos\theta \tag{6}$$

ω being the wetted angle.

It is convenient to rewrite Eqs. (1)–(4) in a more abstract way as

$$\frac{\partial}{\partial t}[\mathbf{w}] + \frac{\partial}{\partial x}[\mathbf{f}(\mathbf{w})] + \mathbf{r}(\mathbf{w}) \frac{\partial}{\partial x}[P] = \mathbf{q}(\mathbf{w}) \tag{7}$$

where the vector

$$\mathbf{w}^{\mathrm{T}} = (\rho_G R_G; \rho_L R_L; \rho_G R_G V_G; \rho_L R_L V_L) \tag{8}$$

encapsulates conservative variables, as a function of which the vectors

$$\mathbf{f}^{\mathrm{T}} = (\rho_G R_G V_G; \rho_L R_L V_L; \rho_G R_G V_G^2 + R_G \Delta P_G; \rho_L R_L V_L^2 + R_L \Delta P_L) \tag{9}$$

$$\mathbf{r}^{\mathrm{T}} = (0; 0; R_G; R_L) \tag{10}$$

$$\mathbf{q}^{\mathrm{T}} = (0; 0; \tau_G + \tau_i - \rho_G R_G g \sin\theta; \tau_L - \tau_i - \rho_L R_L g \sin\theta) \tag{11}$$

are computed. It is also possible to transform (7) into the quasi-linear form

$$\frac{\partial}{\partial t}[\mathbf{w}] + \mathbf{A}(\mathbf{w}) \frac{\partial}{\partial x}[\mathbf{w}] = \mathbf{q}(\mathbf{w}). \tag{12}$$

Under appropriate conditions (Masella, 1997), e.g. if

$$|V_G - V_L| \prec c_m \tag{13}$$

where c_m is a pseudo-sound-velocity of the mixture, the matrix $\mathbf{A}(\mathbf{w})$ has four real eigenvalues $\lambda_1(\mathbf{w}) \leq \lambda_2(\mathbf{w}) \leq \lambda_3(\mathbf{w}) \leq \lambda_4(\mathbf{w})$, as well as a base of eigenvectors. This property is commonly known as *hyperbolicity*. Note that, should the static head terms quantities ΔP_G and ΔP_L be missing in Eq. (3) and Eq. (4), then hyperbolicity would be lost as soon as $V_G \neq V_L$.From the standpoint of physics, the extreme eigenvalues λ_1 and λ_4 are associated to acoustic waves and therefore can be very large, especially when the mixture is mainly composed of liquid. The medium eigenvalues λ_2 and λ_3 are associated to void fraction waves, and their orders of magnitude are about those of fluid velocities.

2.2. Numerical scheme

The resolution algorithm is based on a finite volume method, adapted to the non-conservative form Eq. (12). The reader is referred to Masella's thesis (1997) for a more detailed description of the numerical implementation.

Let us divide the pipeline into a sequence of uniform cells $M_i = [x_{i-1/2}, x_{i-1/2}]$, the length of each of them being Δx. The unknowns are located at the center of the cells: let $\mathbf{w}_i$ be the one associated to the cell M_I. Discretization in space reads

$$\frac{d}{dt}[\mathbf{w}_i] + \frac{\mathbf{h}_{i+1/2} - \mathbf{h}_{i-1/2}}{\Delta x} + \mathbf{r}_i \frac{P_{i+1/2} - P_{i-1/2}}{\Delta x} = \mathbf{q}_i \tag{14}$$

where $\mathbf{h}_{i+1/2}$ and $P_{i+1/2}$ are obtained via a linearized Riemann problem at the interface $x_{i+1/2}$. This simplified Riemann problem, defined from the surrounding states $\mathbf{w}_i$ and $\mathbf{w}_{i+1}$, involves a rough Godunov solver and is referred to as the VFRoe solver (Masella et al., 1996).

The time discretization is explicit with respect to the medium eigenvalues and linearly implicit with respect to the extreme eigenvalues.

One of the trickiest problems here is to deal with the boundary conditions. Usually, two inlet mass flowrates and one outlet pressure are imposed. However, if $\lambda_1(\mathbf{w}) < \lambda_2(\mathbf{w}) \leq \lambda_3(\mathbf{w})$ at the inlet, then a further inlet data has to be supplied. At first sight, a condition on the gas volumetric fraction R_G or on the gas mass fraction $\alpha_G = \rho_G R_G / (\rho_G R_G + \rho_L R_L)$ seems to be relevant. Nevertheless, it comes as a surprise that such a choice does not always give rise to acceptable results, and in reality, the source terms must be taken into account.

As a matter of fact, most two-fluid type codes impose either a von Neuman type boundary condition (De Henau and Raithby, 1995) such as

$$\frac{\partial}{\partial x}[R_L] = 0 \tag{15}$$

Others merely extrapolate the value of the liquid fraction. The staggered mesh approach used in OLGA, with velocities defined at the mesh boundaries and pressure and void fraction defined within the cells, allows avoiding the specification of an extra boundary condition.

A careful investigation into different terms in Eq. (3) and Eq. (4) reveals that, in slow transients, the prevailing terms are the pressure drop and the source terms. When all remaining terms are neglected, Eq. (3) and Eq. (4) degenerate into

$$\tau_G + \tau_L - (\rho_G R_G + \rho_L R_L) g \sin\theta - \frac{\partial}{\partial x}[P] = 0 \tag{16}$$

$$R_G(\tau_L - \tau_i - \rho_L R_L g \sin\theta) - R_L(\tau_G + \tau_i - \rho_G R_G g \sin\theta) = 0 \tag{17}$$

This suggests directly imposing Eq. (16) as the third boundary condition at the inlet.

The next two figures illustrate what has just been said about boundary conditions. Two numerical runs were performed for a pipe of length $L = 10\,000$ m. At the inlet, the flowrates are 10 kg/s (liquid) and 0.1 kg/s (gas). At the outlet, the pressure is maintained at 1 bar. Since three eigenvalues are positive at the inlet, a third boundary condition is required. We attempt to impose $R_G = 0.6$.

In the first run, the diameter is equal to $D = 0.25$ m, which corresponds to large friction terms. It can be seen from Fig. 1 that the inlet value $R_G = 0.6$ is immediately dissipated and as a consequence, does not exercise any influence over the inner state of the mixture. This phenomenon is not sensitive to the mesh size.

In the second run, the diameter is increased to $D = 0.75$ m, so as to reduce the magnitude of friction terms. From Fig. 2, it is now obvious that the inlet value $R_G = 0.6$ is perfectly compatible with the inner state.

3. The drift-flux model

The Drift Flux Model is derived from the Two-Fluid Model by neglecting the static head terms ΔP_G and ΔP_L in the last two Eq. (3) and Eq. (4) and replacing the two momentum equations by their sum. The main advantages of this 3-equation model are:

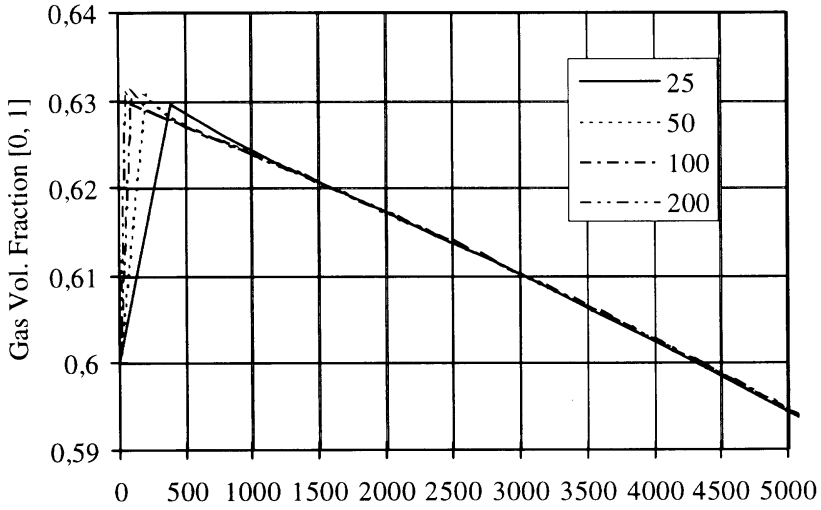

Fig. 1. Profile in space of the gas volumetric fraction for several mesh sizes, with $D = 0.25$ m (zoom up to 5000 m).

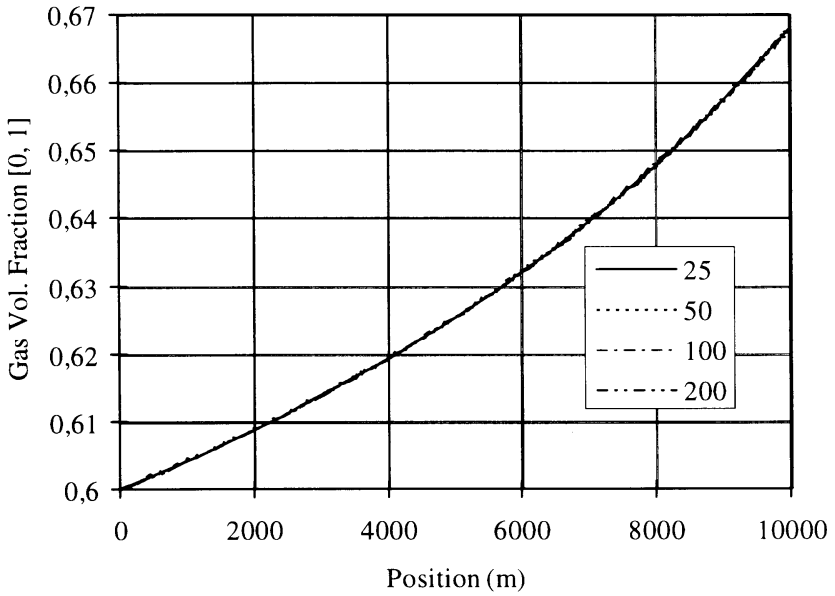

Fig. 2. Profile in space of the gas volumetric fraction for several mesh sizes, with $D = 0.75$ m.

- the equations are in conservative form, which makes it easier to discretize by finite volume methods;
- the interfacial friction term τ_i is cancelled out in the momentum equation, although it appears in an additional algebraic relation called *slip law*;
- one does not have to work out a third boundary condition at the inlet;
- it is generally hyperbolic depending on the form of the *slip law*.

3.1. Transport equations

Adding (3) and (4) together yields

$$\frac{\partial}{\partial t}[\rho_G R_G V_G + \rho_L R_L V_L] + \frac{\partial}{\partial x}[\rho_G R_G V_G^2 + \rho_L R_L V_L^2 + P] = \tau_G + \tau_L - (\rho_G R_G + \rho_L R_L)\sin\theta \tag{18}$$

The interfacial exchange term τ_i is no longer present in the above equation. This leads us to consider DFM, a new model which consists of three partial differential equations, i.e. Eq. (1), Eq. (2) and Eq. (18). In order for DFM to be cast into the strictly conservative form

$$\frac{\partial}{\partial t}[\mathbf{w}] + \frac{\partial}{\partial \mathbf{x}}[\mathbf{f}(\mathbf{w})] = \mathbf{q}(\mathbf{w}), \tag{19}$$

where the flux and the source

$$\mathbf{f}^{\mathrm{T}} = (\rho_G R_G V_G;\ \rho_L R_L V_L;\ \rho_G R_G V_G^2 + \rho_L R_L V_L^2 + P) \tag{20}$$

$$\mathbf{q}^{\mathrm{T}} = (0;\ 0;\ \tau_G + \tau_L - (\rho_G R_G + \rho_L R_L) g \sin\theta \tag{21}$$

are to depend only on

$$\mathbf{w}^{\mathrm{T}} = (\rho_G R_G;\ \rho_L R_L;\ \rho_G R_G V_G + \rho_L R_L V_L), \tag{22}$$

it is necessary to introduce an algebraic relation called *closure law* or slip model.

In stratified flow, the slip relation is obtained by combining the two momentum conservation Eq. (3) and Eq. (4) in such a fashion that the pressure gradient vanishes. By neglecting derivatives with respect to time, static head and inertia terms in this combination, we end up with

$$\frac{\tau_G}{\tau_G} - \frac{\tau_L}{\tau_L} + \frac{\tau_i}{R_G R_L} + (\rho_G - \rho_L) g \sin\theta = 0. \tag{23}$$

For other flow regimes, the closure law may be much more sophisticated.

It is mathematically equivalent to rewrite Eq. (19) under the quasi-linear form

$$\frac{\partial}{\partial t}[\mathbf{w}] + \mathbf{A}(\mathbf{w}) \frac{\partial}{\partial x}[\mathbf{w}] = \mathbf{q}(\mathbf{w}), \tag{24}$$

in which $\mathbf{A}$ is the Jacobian matrix of $\mathbf{f}$ with respect to $\mathbf{w}$. If hyperbolicity holds, there exist three eigenvalues $\lambda_1 \leq \lambda_2 \leq \lambda_3$ and a base of eigenvectors. As is the case for TFM, the extreme eigenvalues are associated to acoustic waves, whereas the medium eigenvalue is associated to a void fraction wave.

3.2. Numerical scheme

In this section, the basic ideas of the numerical scheme are outlined. Further details are to be found in Faille and Heintzé (1996).

Once again, let us divide the pipeline into regular cells $M_i = [x_{i-1/2}, x_{i+1/2}]$, the size of which is denoted by Δx. The unknowns are located at the center of the cells: let $\mathbf{w}_i$ be the one associated to the cell M_i. Discretization in space reads

$$\frac{d}{dt}[\mathbf{w}_i] + \frac{\mathbf{h}_{i+1/2} - \mathbf{h}_{i-1/2}}{\Delta x} = \mathbf{q}_i \tag{25}$$

with

$$\mathbf{h}_{\mathrm{i}+1/2} = \frac{1}{2}[\mathbf{f}(\mathbf{w}_{\mathrm{i}}) + \mathbf{f}(\mathbf{w}_{\mathrm{i}+1})] - \frac{1}{2}\mathbf{D}_{\mathrm{i}+1/2}(\mathbf{w}_{\mathrm{i}+1} - \mathbf{w}_{\mathrm{i}}) \tag{26}$$

In this formula, $\mathbf{D}_{i+1/2}$ is a diffusion matrix that has to be built up from $\mathbf{w}_i$ and $\mathbf{w}_{i+1}$. Extension to second order accuracy is achieved via the MUSCL strategy. Eqs. (25) and (26) may appear to be a little simple-minded, but in reality, standard Godunov-type schemes using

approximate Riemann solvers (Godlewski and Raviart, 1996) at sides $x_{i+1/2}$ lead to even poorer results. This is quite a puzzling feature of DFM.

The time discretization is explicit with respect to the medium eigenvalue and linearly implicit with respect to the extreme eigenvalues.

4. The no-pressure-wave model

Experience with numerical simulations has shown that, in most transients of interest to the oil and gas transport industry, pressure waves do not have a strong effect on the initiation and transport of void waves. Hence, in a bolder step toward simplification, we would like to rule out the very existence of acoustic waves from the model equations.

4.1. Transport equations

Preliminary numerical investigations into the order of magnitude of different terms in Eq. (18) suggest that, in slow transients, it is legitimate to neglect the inertia terms. Doing so amounts to replacing the mixture momentum Eq. (18) by a local static force balance

$$\frac{\partial}{\partial x}[P] = \tau_G + \tau_L - (\rho_G R_G + \rho_L R_L) g \sin\theta. \tag{27}$$

The NPW model is made up of Eq. (1), Eq. (2) and Eq. (27). The three partial differential equations are complemented by an algebraic *slip law*.

Let us introduce superficial velocities

$$U_G = R_G V_G \tag{28}$$

$$U_L = R_L V_L \tag{29}$$

$$U_S = U_G + U_L \tag{30}$$

and let us consider

$$\mathbf{v}^{\mathrm{T}} = (R_G, P, U_S) \tag{31}$$

as principal unknowns. This choice of variables turns out to be very handy for tackling the limiting case of incompressible flows. The equations of NPW can be summarized as

$$\frac{\partial}{\partial t}[\mathbf{e}(\mathbf{v})] + \frac{\partial}{\partial x}[\mathbf{f}(\mathbf{v})] = \mathbf{q}(\mathbf{v}) \tag{32}$$

with

$$\mathbf{e}^{\mathrm{T}} = (\rho_G R_G;\ \rho_L R_L;\ 0) \tag{33}$$

$$\mathbf{f}^{\mathrm{T}} = (\rho_G R_G V_G;\ \rho_L R_L V_L;\ P) \tag{34}$$

$$\mathbf{q}^{\mathrm{T}} = (0; 0; \tau_G + \tau_L - (\rho_G R_G + \rho_L R_L) g \sin\theta) \tag{35}$$

The slip law is formally expressed as

$$U_G = \Psi(R_G, P, U_S) \tag{36}$$

where the function Ψ may admit the pipe angle of inclination θ as a parameter.

Viviand (1996) shows that this model is a good approximation of the DFM as long as the phasic velocities are small compared to the sound wave velocities, which is true for most applications. He also proves that NPW always has a single finite eigenvalue, equal to

$$\lambda(\mathbf{v}) = \frac{\partial}{\partial R_G}[\Psi(\mathbf{v})]. \tag{37}$$

The characteristic equation associated to this eigenvalue can be written as

$$\mathbf{I}^T(\mathbf{v}) \cdot \left\{ \frac{\partial}{\partial t}[\mathbf{v}] + \lambda \frac{\partial}{\partial x}[\mathbf{v}] \right\} = \mathbf{I}^T(\mathbf{v}) \cdot \mathbf{q}(\mathbf{v}) \tag{38}$$

$\mathbf{I}^T(\mathbf{v})$ being an appropriate left eigenvector. Besides, there exists an algebraically-double eigenvalue equal to ∞. On this ground, the model is qualified as *mixed hyperbolic/parabolic*. The number of characteristic equations associated with ∞ is usually one, i.e. Eq. (27), but may reach two for special thermodynamic laws.

4.2. Numerical scheme

In this section, the basic ideas of the numerical scheme are outlined. Further details are to be found in Patault and Tran (1996).

The pipeline is divided into regular cells $M_i = [x_{i-1/2}, x_{i+1/2}]$, the size of which is denoted by Δx. The unknowns are located at the center of the cells: let $\mathbf{v}_i$ be the one associated to the cell M_i. Unlike the two previous schemes, the NPW equations are discretized in a centered way at the sides $x_{i+1/2}$. In other words,

$$\frac{1}{2}\frac{d}{dt}[\mathbf{e}(\mathbf{v}_i) + \mathbf{e}(\mathbf{v}_{i+1})] + \frac{\mathbf{f}(\mathbf{v}_{i+1}) - \mathbf{f}(\mathbf{v}_i)}{\Delta x} = \frac{1}{2}[\mathbf{q}(\mathbf{v}_i) + \mathbf{q}(\mathbf{v}_{i+1})] \tag{39}$$

Discretization in time of Eq. (39) is totally implicit. The final scheme is first order accurate in time, and second order in space.

Eq. (39) has to be modified over a cell across which the sign of the eigenvalue λ changes, to track shocks and rarefaction waves. An algorithm, inspired from Chattot and Malet (1987), is set up to build the system of equations to be solved at each time step, according to the characteristic velocity sign configuration.

Table 1
Definition of the reference test case

Pipe geometry	Length	420 m
	Diameter	3″
	Configuration	Horizontal
Transient scenario	Inlet gas flowrate	From 0.0048 to 0.0354 kg/s^2 in 20 s
	Inlet liquid flowrate	0.191 kg/s^2
	Outlet pressure	1.68 bar
Fluid definition and properties	Composition	Air/Kerosene
	Gas density	2.418 kg/m^3
	Liquid density	813 kg/m^3
	Gas viscosity	0.76 10^{-5} m^2/s
	Liquid viscosity	0.22 10^{-5} m^2/s
	Superficial tension	0.03 N/m^2

5. Comparisons of the models

To compare the response of the three models, we first define a reference test case. This is done in Table 1. For this test case, we display the theoretical response of each transport model. By theoretical response, we mean the limit response obtained by decreasing the mesh size Δx to 0.

Next, we compare the response of the three codes to the experimental measurements. We also plot the computing time versus the accuracy for each the model response.

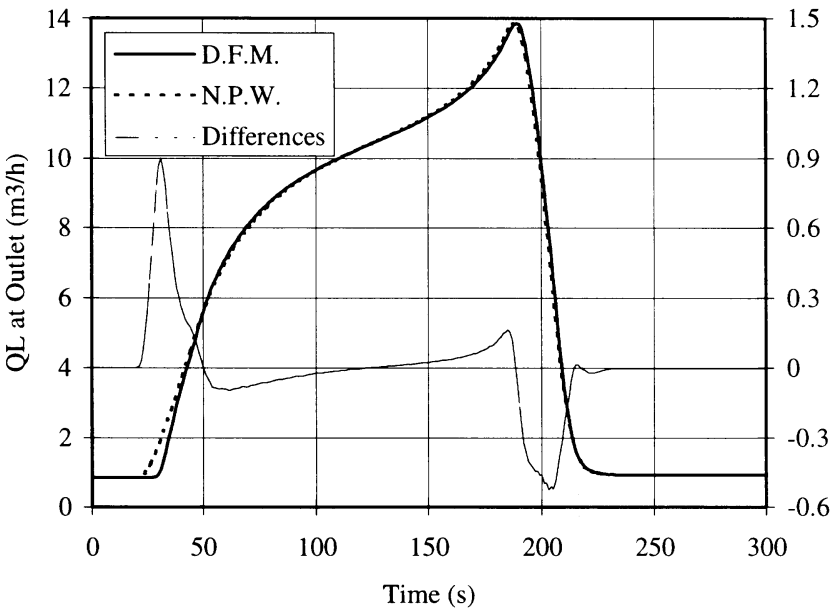

Fig. 3. Comparison between DFM and NPW on outlet liquid flow rate.

Finally, we look at the response of NPW and DFM on a scenario giving rise to the severe slugging phenomenon. On this case, the differences in responses are explained by arguments involving the transport models and the numerical schemes.

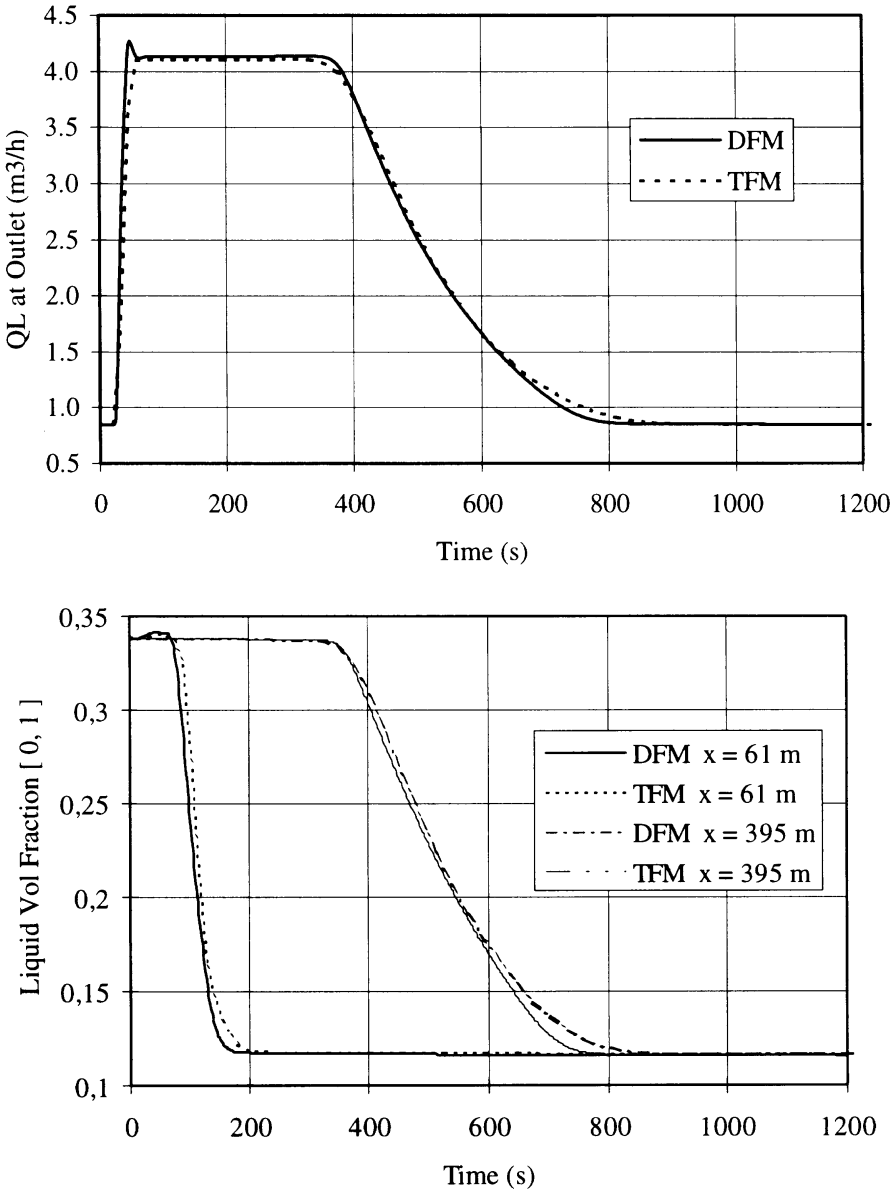

Fig. 4. (a) Comparison between DFM and TFM on outlet liquid flow rate. (b) Comparison between DFM and TFM on liquid volume fraction.

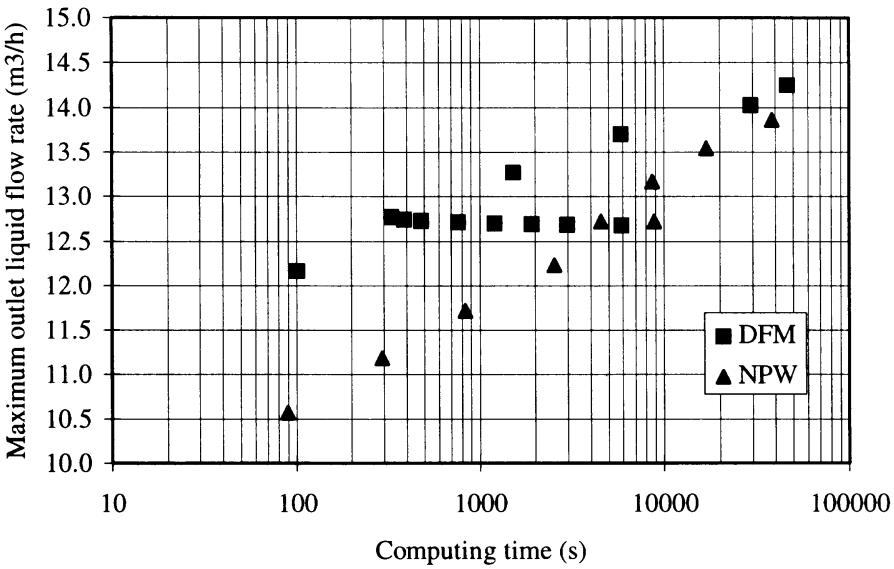

Fig. 5. Comparison of computing efficiency between DFM and NPW model.

5.1. Transient response of models for reference case

Let us start by describing the actual values of parameters for the reference case.

Fig. 3 compares the transient response of DFM with NPW for $\Delta x = 2$ m. Below this value of the mesh size, no significant improvement in the accuracy of the solution for each model is observed. Therefore, we assimilate the curves to the "analytical" solutions of the models.

To avoid discrepancies due to the slip model, we use in both cases a Zuber and Findlay (1965) slip model, which is an alternative to the slip model defined in Eq. (23). The curves in Fig. 3 exhibit very little differences in the transient response of the two models. This corroborates the theoretical prediction by Viviand, according to which pressure waves play a minor role on the propagation of the liquid.

Fig. 4 compares the transient responses of DFM and TFM, using a stratified slip model as specified in Eq. (23). One must bear in mind the fact that TFM includes a pressure difference term due to the liquid fraction gradient, which is not included in DFM.

Although the transient imposed on the system is quite rapid (a 20 s ramp in inlet gas flow rate), the responses of DFM and TFM are quite similar. This result tends to indicate that TFM's decoupling of the phase velocities does not significantly affect the transient response of the model. In other words, it is the source terms that actually control the transient response.

In Fig. 5 we try to characterise the computing efficiency of the different codes. For this purpose, we define the "computing efficiency" as the relation between the computing time and the peak height in the liquid outlet flowrate. This maximum in the liquid outlet flowrate is important for pipeline design because it characterises the outlet liquid flowrate surge into the

separator following and increase in the inlet gas flowrate. The estimation of this liquid surge will eventually control the outlet separator volume design recommendation.

The diagram in Fig. 5 shows that for a given accuracy, the mixed explicit/implicit resolution used in the DFM code is faster than the implicit resolution in the NPW code.

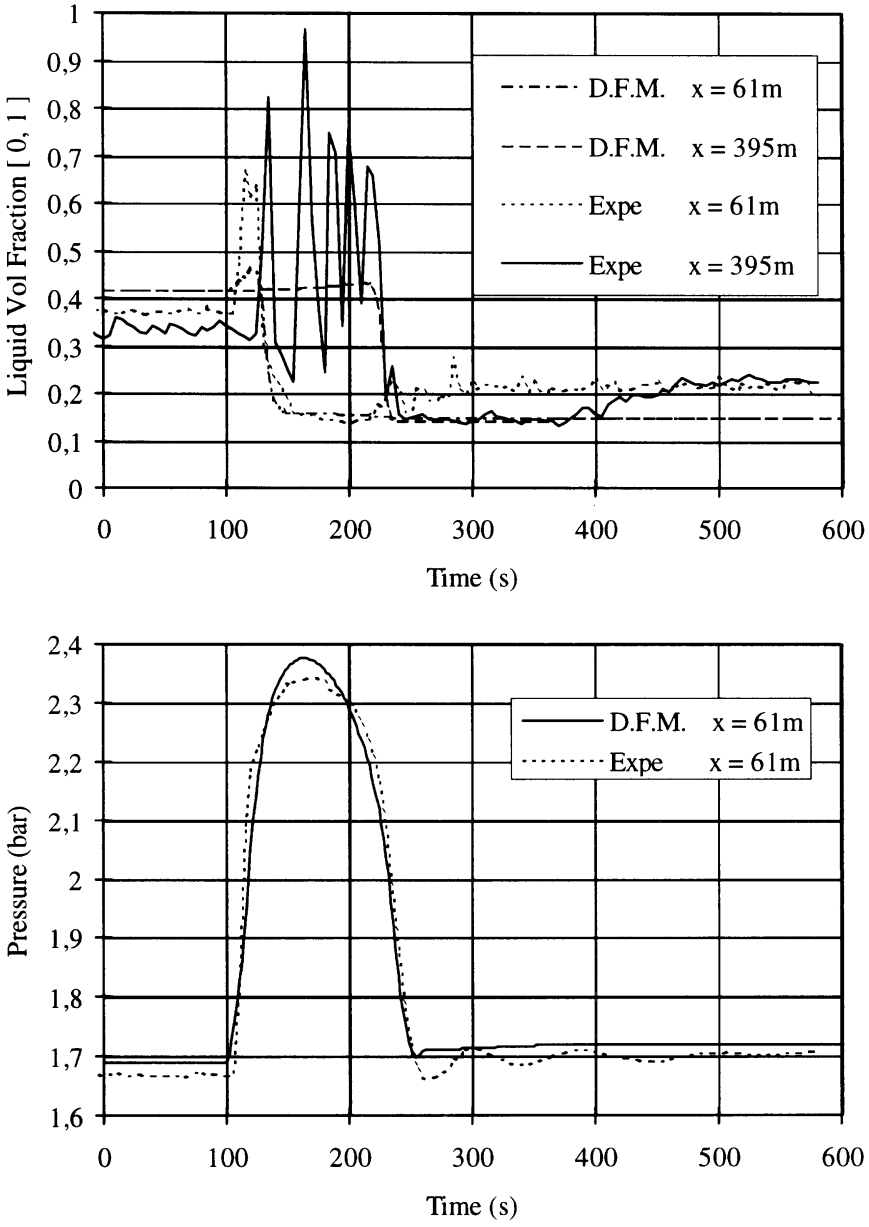

Fig. 6. (a) Comparison between measured and computed liquid fraction using DF model. (b) Comparison between measured and computed pressure using DF model.

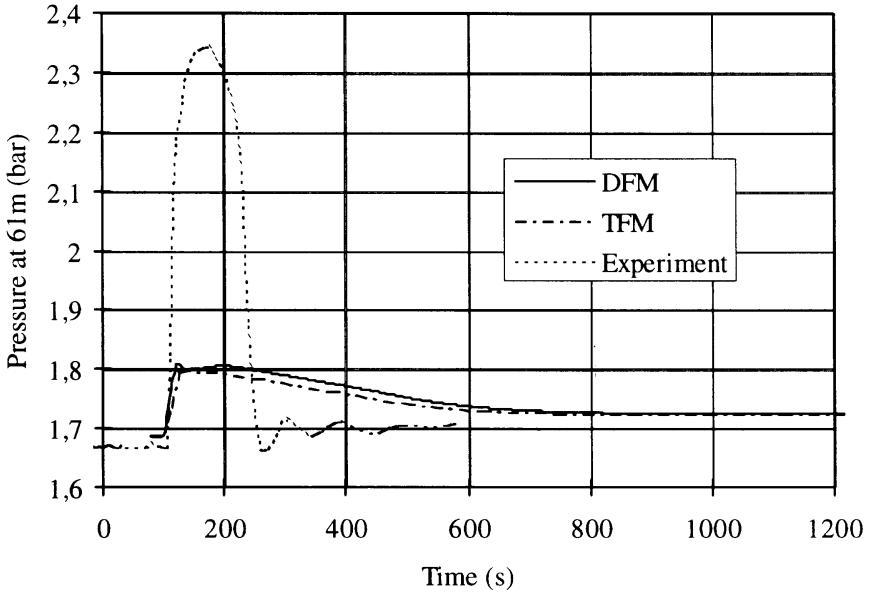

Fig. 7. Comparison between experimental and computed pressure using the DFM and TFM models with an imposed stratified configuration.

5.2. Comparison with experimental data

Next we compare the code responses with experimental data (Vigneron, 1995) taken for the same test case. Fig. 6 compares the experimental results with the transient response of the DFM using a *slip model* which takes into account the different flow regimes which can possibly be encountered.

The large amplitude oscillations observed during the transient period signal the occurrence of the slug flow regime. The recognition of this flow regime has important implications on the pressure drop calculation.

Table 2
Definition of the severe slugging test case

Pipe geometry	Length	60 m and 14 m
	Diameter	2″
	Configuration	Horizontal and vertical
	Inlet gas flowrate	0.000196 kg/ s^2
Transient scenario	Inlet liquid flowrate	0.07854 kg/s^2
	Outlet pressure	1.0 bar
Fluid definition and properties	Composition	Air/Kerosene
	Gas density	1.0 kg/m^3
	Liquid density	1000 kg/m^3
	Gas viscosity	1.5 10^{-5} m^2/s
	Liquid viscosity	1.5 10^{-6} m^2/s
	Superficial tension	0.07 N/m^2

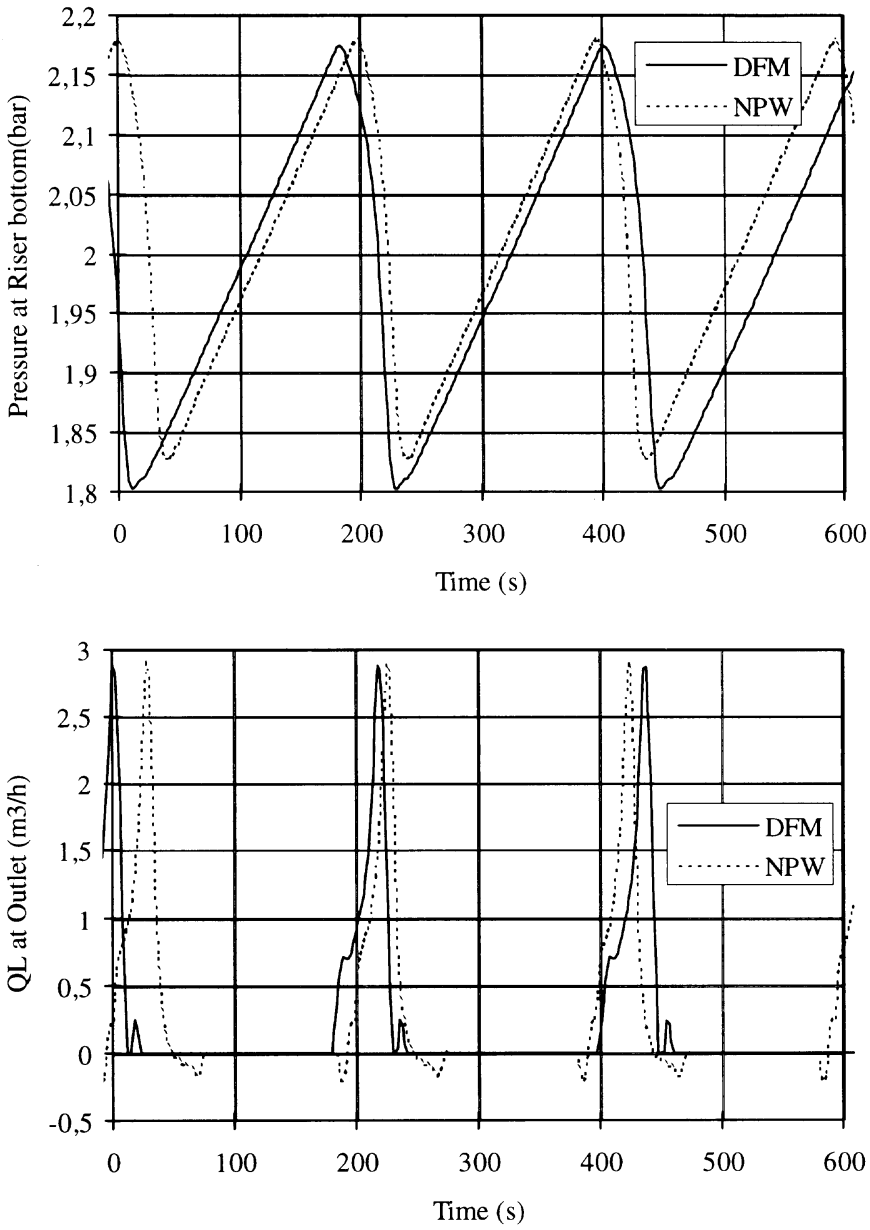

Fig. 8. (a) Comparison between the DFM and the NPW models on pressure at riser bottom for a severe slugging case. (b) Comparison between the DFM and the NPW models on outlet liquid flow rate for a severe slugging case.

Fig. 7 compares the same experimental results with the transient response of the DFM and TFM with the slip model assuming a stratified flow configuration.

From Fig. 6b and Fig. 7, one can notice the important effect of the flow regime prediction and subsequent slip relation on the pressure transient response of the model.

5.3. Severe slugging case

Lastly, we compare the DFM and the NPW models on a severe slugging test case.

Table 2 defines the severe slugging test case. Fig. 8 shows the comparison between the two codes. Slight differences are observed in the period and amplitude of oscillations. However these can be attributed to the differences in treatment of the outlet boundary conditions. As can be seen, the DFM solution algorithm at the outlet does prevent liquid from going back into the pipeline during the reflux period. This problem is resolved by introducing a fictitious cell at the outlet in which we assume single phase gas flow.

6. Conclusion

Extensive numerical tests have been carried out in order to compare the analytical response of the three following models:

- a Two Fluid Model with one momentum equation for each phase;
- a Drift Flux Model with only one momentum equation for the mixture;
- a No Pressure Wave model reducing the momentum equation to a force balance.

On one hand, different hydrodynamic slip laws have been incorporated into these models. The results clearly show that the choice of the former has an critical effect on the dynamic response of the latter.

On the other hand, comparison between the different transport models confirms the fact that the source terms in the momentum equation do dominate the transient response of the model. This holds true for all models, but becomes overwhelmingly apparent in the case of TFM.

The computing efficiency as defined from the end user's perspective, that is, the peak in outlet liquid flowrate subsequent to an increase in the inlet gas flowrate, has been analyzed for DFM and NPW. For a given accuracy, the DFM explicit/implicit resolution is faster than the implicit resolution employed in the NPW code.

Acknowledgements

We gratefully acknowledge the contributions of H. Viviand for his analysis of the NPW model and of S. Patault for its numerical implementation. We also wish to thank J. Brill (TUFFP) for allowing us to use one of his experimental datasets as a reference test case. This work was performed in the framework of the TACITE project supported by the Institut Français du Pétrole, Elf Aquitaine, and Total Exploration Production.

References

Bendiksen, K., Brandt, I., Jacobsen, K.A., Pauchon, C. 1987. Dynamic simulation of multiphase transportation systems. Multiphase Technology and Consequences for Field development Forum, Stavanger, Norway.

Bendiksen, K., Malnes, D., Moe, R., Nuland, S., 1991. The dynamic two-fluid model OLGA: theory and application. SPE Production Engineering 6, 171–180.

Black, P.S., Daniels, L.C., Hoyle, N.C., Jepson, W.P., 1990. Studying transient multiphase flow using the Pipeline Analysis Code (PLAC). Journal of Energy Resources Technology 112, 25–29.

Chattot, J.J., Malet, S. 1987. A box-scheme for the Euler equations. In: Non-linear hyperbolic problems, Carasso, C., Raviart, P.A., Serre, D., (Eds.), Lecture Notes in Mathematics, vol. 1270, Springer-Verlag.

De Henau, V., Raithby, G.D., 1995. A transient two-fluid model for the simulation of slug flow in pipelines, 1—Theory. Int. J. Multiphase Flow 21, 335–349.

Faille, I., Heintzé, E. 1996. Rough finite volume schemes for modelling two-phase flow in a pipeline. In: Proceedings of the CEA, EDF, INRIA course "Méthodes numériques pour les écoulements diphasiques". INRIA Rocquencourt, France.

Godlewski, E., Raviart, P.A. 1996. Numerical approximation of hyperbolic systems of conservation laws. Springer-Verlag, New York.

Masella, J.M. 1997. Doctoral thesis, Université de Pierre et Marie Curie, Paris, France.

Masella, J.M., Faille, I., Gallouët T. 1996. On a rough Godunov scheme. Submitted.

Patault, S., Tran, Q.H. 1996. Modèle et schéma numérique du code TACITE-NPW. Technical Report 42415, Institut Français du Pétrole, France.

Pauchon, C., Dhulesia, H., Lopez, D., Fabre, J. 1993. TACITE: A comprehensive mechanistic model for two-phase flow. In: Proceedings of the 6th International Conference on Multiphase Production, Cannes, France.

Pauchon, C., Dhulesia, H., Binh-Cirlot, G., Fabre, J. 1994. TACITE: A transient tool for multiphase pipeline and well simulation. SPE Annual Technical Conference, SPE 28545,New Orleans, LA, USA, pp. 25–28.

Taitel, Y., Shoham, O., Brill, J.P., 1989. Simplified transient solution and simulation of two-phase flow in pipelines. Chem. Eng. Sci. 44, 1353–1359.

Viviand, H. 1996. Modèle simplifié d'écoulement dans les conduites pétrolières. Technical Report RSY.43.069.02., Principia, France.

Vigneron, F. 1995. Analysis of imposed two-phase flow transients in horizontal pipelines, Part 1—Experimental results. Research Report, Tulsa University Fluid Flow Project, USA.

Zuber, N., Findlay, J.A., 1965. Average volumetric concentration in two-phase flow systems. J. Heat Transfer Series C 87, 453–458.